Electronic Materials Letters, Vol. 2, No. 3 (2006), pp. 161-166

Effects of Zn Addition on the Interface Microstructure and Drop Reliability of Sn-3.5Ag Solder on Cu pads

Young-Kun Jee, Yong-Ho Ko, Yoon-Chul Sohn, and Jin Yu

Department of Materials Science and Engineering, KAIST, 373-1 Guseong-dong, Yuseong-gu, Daejeon 305-701, Korea

Varying amounts of Zn(1, 3, and 7wt%) were added to Sn-3.5Ag solder on a Cu pad, and the effects of Zn on the interface microstructure and drop resistance were investigated. Results indicate that addition of 3wt% Zn increased the number of drops to failure (N_f) by about two times and that aging generally deteriorated the drop reliability. The beneficial role of Zn was ascribed to the suppression of Cu_6Sn_5 at the joint interface. Effects of aging were assumed to lead to the formation of double IMC layers (0Zn, 1Zn) and decomposition of Ag_5Zn_8 into brittle Ag_3Sn and Cu_6Sn_5.

Key words: lead-free solder, Zn effect, intermetallic compound, drop test

1. INTRODUCTION

With worldwide legislative moves to eliminate the use of Pb in commercial electronics[1], Sn-Ag, Sn-Cu, Sn-Ag-Cu, and Sn-Zn solder alloys have been considered as substitutes to lead-free solder materials[2-5]. In particular, lead-free solders bearing Zn have received considerable attention, as Zn is known to improve the mechanical reliability of solder alloys. The Sn-9Zn eutectic alloy is a candidate lead-free solder due to its low melting point (198 ^oC), excellent mechanical properties, and low cost[6,7], despite that there remain some problems such as poor wettability and easy oxidation[4]. The addition of Ag to Sn-Zn solder is known to improve the solder's oxidation resistance and wetting behavior[8,9]. The solder joint microstructure is significantly affected by underlying UBMs, and the intermetallic compounds (IMC) of Sn-Zn solder over a Cu pad are Cu-Zn IMCs, not Cu-Sn IMCs[10-12]. In the case of Sn-9Zn/Cu, three sub-layers, β'-CuZn, γ-Cu_5Zn_8, and an unknown Cu-Zn phase, are formed. Furthermore, rapid thickening of γ-Cu_5Zn_8 during aging was reported to lower the joint strength significantly[10,11]. Chang[13] found that planar type Cu_6Sn_5, which formed after soldering, subsequently transformed to scallop type Cu_5Zn_8 after aging at 180 ^oC for 250 hr. The correlation between the interface microstructure and the mechanical reliability of Sn-Zn or Sn-Ag-Zn alloys over Cu or Ni(P) pads are not yet well known.

A new dimension to the issue of solder joint reliability has emerged as packaging technology is driven by handheld microelectronics products such as cellular phones and PDAs. They are prone to accidental drops, and the resistance of solder joints to drop impact thus becomes more important[14]. Consequently, extensive drop tests are being conducted using various Pb-free solders, and effects of surface finishes such as ENIG and Cu on the solder joint strength are being investigated extensively[15-21]. In the present work, effects of Zn addition on the microstructure and drop reliability of Sn-3.5Ag solder on Cu finishes were investigated, and the interface microstructure was correlated to the drop failure resistance.

*Corresponding author: charisma888@kaist.ac.kr

2. EXPERIMENTAL PROCEDURES

Sn-3.5Ag-Zn solder balls with varying Zn content(0, 1, 3, and 7 wt%; in the following each alloy is denoted as 0Zn, 1Zn, 3Zn, and 7Zn, respectively) were prepared by mixing high purity metal powders (99.99%) followed by melting in a quartz tube (10^{-3} torr vacuum), cold stripping, punching disks, and dropping in a high temperature medium[22].

Drop test specimens with the geometry given in Fig. 1 were fabricated by connecting two PCBs (FR4, 3.1mm thick) with solder balls. Surface finishes of PCB were Cu (35 μm) metallization. Dimensions of the top and bottom substrates were 1×1 and 4×10 cm^2, respectively. To make a drop specimen, 16 solder balls with respective diameter of 760 um were mounted on the bottom PCB and reflowed. After the attachment of the top PCB, the whole assembly was reflowed once more. Thus, the bottom part of the solder

underwent one reflow more than the top part. Solder reflow was made in an oven with a maximum temperature of 258 °C, and the duration of stay above the melting point of Sn-3.5Ag was about 90 seconds. To stabilize the reflowed solder microstructure, specimens were aged after reflow for 500 hr at 150 °C.

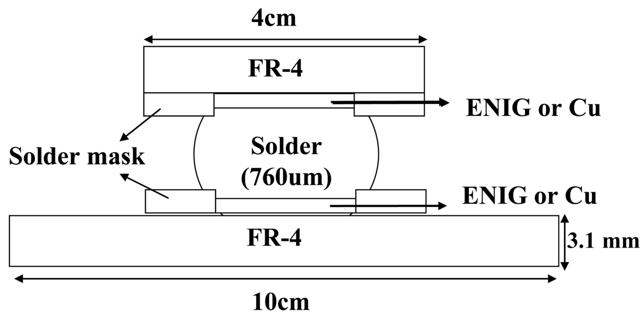

Fig. 1. Schematic diagram of drop test specimen.

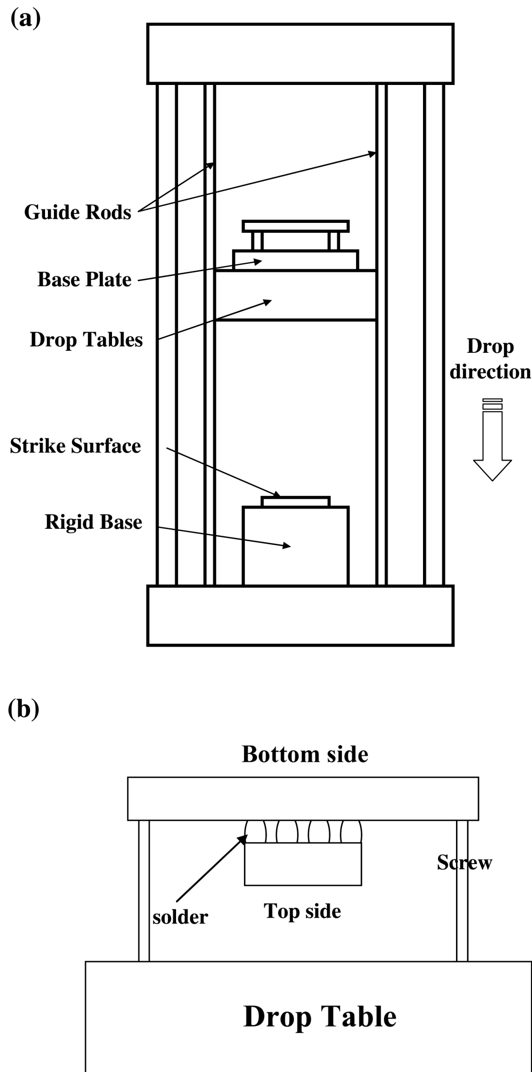

Fig. 2. Setup of drop test. (a) Overview of drop tester (b) Magnified view of drop sample.

Before the drop test, the board assembly was flipped upside down and fixed to the drop table, as shown in Fig. 2(b). The shock loading was set according to JESD22-B110 by adjusting the drop height, and the shock pulse from the drop impact was optimized to a triangular shape with a peak acceleration of 1500G peak for 0.5 ms. The dynamic resistance of daisy-chained solder joints was measured in real-time during the drop test, and the threshold resistance of 20 Ohms (initial resistance: ~60 ohms) was used as a criterion of failure of the daisy chains. When failure did not occur within 250 drops, the drop test was stopped. Before and after the drop test, IMC microstructure and the failure locus of the solder joints were examined by scanning electron microscopy (SEM), focused ion beam (FIB), and energy dispersive X-ray spectroscopy (EDX).

3. RESULTS AND DISCUSSION

3.1. Solder microstructure

SEM micrographs of the as-reflowed and aged Sn-3.5Ag-xZn solders on a Cu pad are given in Figs. 3(a)-(h). Effects of Zn on the solder joint microstructure can be seen by reading the micrographs vertically, while the effect of solid state aging can be found by reading horizontally. When molten solder reacted with the Cu UBM, scallop-type Cu_6Sn_5 developed in the absence of Zn. However, with an addition of 3 wt% Zn, Cu_6Sn_5 at the interface was completely replaced by Cu_5Zn_8 and Ag_5Zn_8, and the latter thickened at the expense of the former with even more Zn. This can be ascribed to the active supply of Ag and Zn from the melt.

The effect of solid state aging of eutectic Sn-3.5Ag solder is to introduce layer type Cu_3Sn underneath Cu_6Sn_5 (cf. Fig. 3(b)). The two layer structure of Cu_6Sn_5 and Cu_3Sn is well known[20]. While a few Kirkendall voids were formed in the Cu_3Sn phase, the degree of voiding was not as severe as that reported elsewhere[20,23]. Rows of Kirkendall voids in the region near the Cu/Cu_3Sn interface are known to degrade the solder joint reliability.

In the case of 1Zn alloy, the as-reflowed microstructure is not substantially different from that of 0Zn alloy (Sn-3.5Ag) except for the presence of Cu_5Zn_8 precipitates in the solder. With further aging, Cu_5Zn_8 formed a continuous IMC layer and thickened while the thickness of the Cu_6Sn_5 layer remained virtually unchanged. This suggests that Cu diffuses into Cu_6Sn_5 but Sn does not and that Cu reacts preferentially with Zn over Sn at 150 °C. Note that 1 wt% Zn suppressed the formation of Cu_3Sn and accompanying Kirkendall voids, thereby improving the mechanical reliability. This is consistent with the report of Kang *et al.*[23], who found that minor Zn alloying (0.7 wt%) modified the interfacial reactions and retarded the Cu_3Sn phase through the accumulation of Zn atoms at the Cu/Cu_3Sn interface.

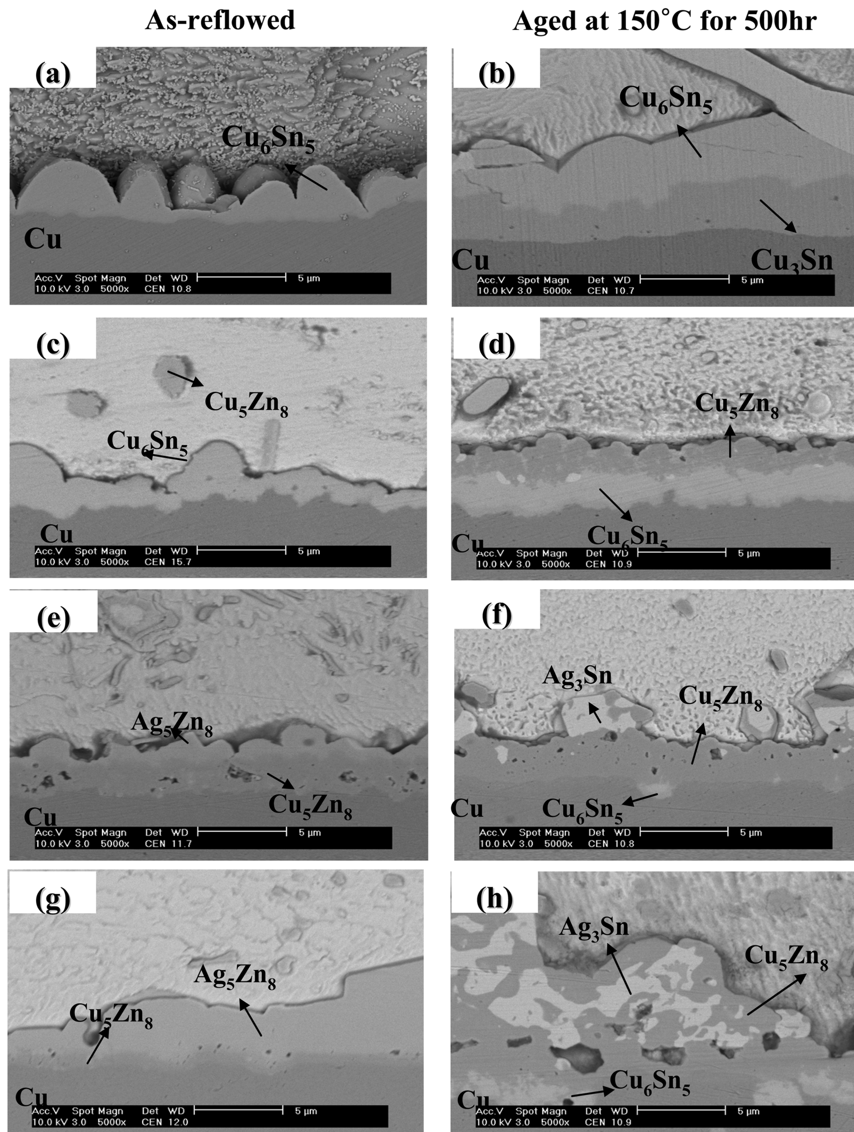

Fig. 3. SEM micrographs of the cross-section of the solder joints on Cu. (a) and (b) Sn-3.5Ag, (c) and (d) Sn-3.5Ag-1.0Zn, (e) and (f) Sn-3.5Ag-3.0Zn, (g) and (h) Sn-3.5Ag-7.0Zn.

Enrichment of Zn at the molten solders/pad interface completely suppressed Cu_6Sn_5 and instead led to the formation of Ag_5Zn_8/Cu_5Zn_8 in the case of the as-reflowed 3Zn speciemen. Since the two Zn-rich IMCs have the same crystal structure, it appears that gradual partitioning of Ag atoms into Cu_5Zn_8 and subsequent precipitation of Ag_5Zn_8 occurred[28]. According to the Cu-Zn and Ag-Zn binary phase diagrams, β'(CuZn or AgZn), γ(Cu_5Zn_8 or Ag_5Zn_8), and ε($CuZn_3$ or $AgZn_3$) phases can form at 250 ^oC[24].

It is worth noting that numerous Kirkendall voids formed in the Cu_5Zn_8 phase of the as-reflowed 3Zn specimen, but it is not clear at present whether this indicates larger diffusion flux of Cu through Ag_5Zn_8 than Ag flux through Cu_5Zn_8. During the isothermal aging, Ag_5Zn_8 transformed into Cu_5Zn_8 and Ag_3Sn, and precipitates of Cu_6Sn_5 were observed inside the Cu layer, presumably by the penetration of Sn into the Cu pad through channels in γ-Cu_5Zn_8[10]. It was suggested by Date[25] that rapid diffusion of Sn along the grain boundaries of γ-Cu_5Zn_8 is responsible for the formation of Cu_6Sn_5 underneath the Cu_5Zn_8 IMC layer.

In the case of the as-reflowed 7Zn specimen, the Ag_5Zn_8 layer grew to be thicker than the Cu_5Zn_8 layer, and there were fewer Kirkendall voids than in the 3Zn specimen. This suggests that higher Zn activity in the molten solder yielded faster reaction kinetics of Ag_5Zn_8. The microstructure of the aged 7Zn alloy is very intriguing. From the position of the Kirkendall voids, which grew larger during the aging treatment, it can be seen that Ag_5Zn_8 decomposed to Ag_3Sn and Cu_5Zn_8, resulting in a mixture of Ag_3Sn and Cu_5Zn_8 precipitates above the voids. The Cu_5Zn_8 phase below the voids

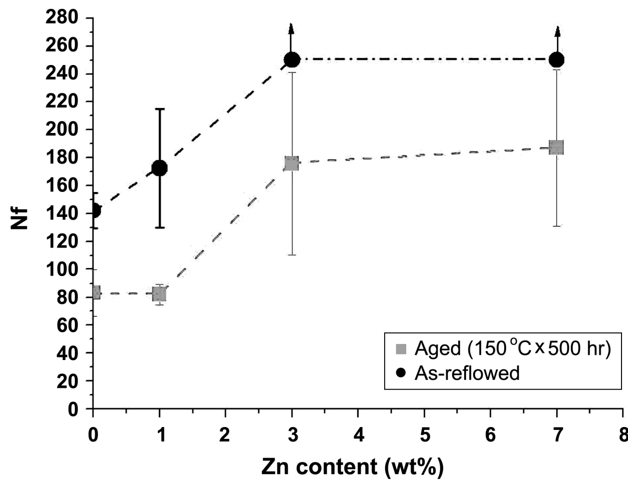

Fig. 4. Mean number of dorp to failure of the board assemblies with lead free solders on Cu metallization.

became much thicker, presumably because Zn diffuses faster than Cu in γ-Cu_5Zn_8[26]. The Cu_5Zn_8/Cu interface became very irregular and precipitation of Cu_6Sn_5 underneath the Cu_5Zn_8 phase increased.

3.2. Drop test results and the failure locus

The number of drops to failure (N_f) is plotted as a function of Zn content in the solder in Fig. 4. As noted in the previous section, a drop specimen was considered to fail when the resistance of the daisy chain dropped to less than one-third of the initial value, and the drop test was stopped when the failure criterion was not met within 250 drops (i.e. $N_f > 250$). Two important observations are made from Fig. 4. First, addition of Zn had beneficial effects on N_f. Whereas one wt% Zn was not effective, 3 wt% Zn raised N_f by about two times. Second, aged specimens showed worse drop reliability than as-reflowed specimens. The beneficial role of Zn

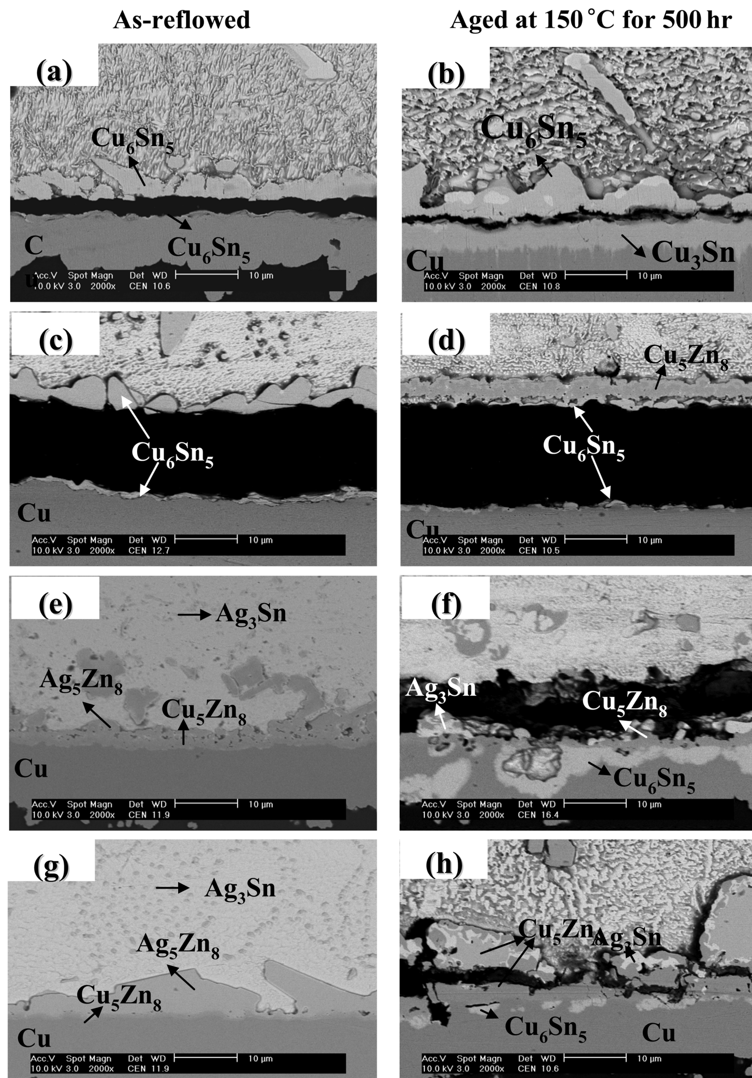

Fig. 5. Brittle fracture images at the interface on Cu. (a) and (b) Sn-3.5Ag, (c) and (d) Sn-3.5Ag-1.0Zn, (e) and (f) Sn-3.5Ag-3.0Zn, (g) and (h) Sn-3.5Ag-7.0Zn.

can be ascribed to the elimination of layer type Cu_6Sn_5 at the solder joint interface. Therefore, as-reflowed specimens of 0Zn and 1Zn alloys with similar Cu_6Sn_5 layer at the interface showed a similar level of N_f. However, the drop failure resistance increased substantially when interfacial Cu_6Sn_5 was suppressed by more than 3 wt% Zn. During the isothermal aging treatment, IMC generally thickened (0Zn, 1Zn and 7Zn specimens) and often formed two IMC layer structures (0Zn, 1Zn specimens), which are detrimental to the joint reliability.

Failure loci of the Sn-3.5Ag-xZn specimens are given in Fig. 5. Except for the as-reflowed 3Zn and 7Zn specimens, all failures occurred through the IMC layer at the solder/pad interface. This is to be expected considering the inherently brittle nature of IMCs. For the as-reflowed 0Zn specimen, failure occurred in the Cu_6Sn_5 IMC layer near the Cu_6Sn_5/Cu interface, due to the scallop-like shape of Cu_6Sn_5 (N_f ~140). Notably, the crack propagated along the Cu_6Sn_5/Cu_3Sn interface in the aged 0Zn specimen at substantially lower N_f (~80). Seperation of the Cu_6Sn_5/Cu_3Sn interface was reported by Jeong[27]. This is related to the presence of Kirkendall voids and the fact that plastic relaxation by the dislocation transmission can be particularly difficult at the IMC interface. The is quite similar to the case of 1Zn specimens, where failure occurred through the Cu_6Sn_5 layer for the as-reflowed (N_f ~170) specimen but near the Cu_5Zn_8/Cu_6Sn_5 interface(N_f ~80) for the aged specimen.

The beneficial role of Zn can be seen in the as-reflowed 3Zn and 7Zn specimens, which did not fail up to 250 drops (cf. Figs. 5(e) and (g)). The 3Zn and 7Zn specimens did not fail despite the presence of Kirkendall voids in Cu_5Zn_8 and at the Ag_5Zn_8/Cu_5Zn_8 interface, respectively. Thus, it appears that Cu_5Zn_8 and Ag_5Zn_8 are quite resistant to brittle fracture. Nonetheless, the aged 3Zn and 7Zn specimens failed at N_f :175 - 190. Since Ag_3Sn and Cu_6Sn_5 are known as brittle phases[29,30], it appears that precipitaion of Ag_3Sn and Cu_6Sn_5 and thickening of the Cu_5Zn_8(7Zn) layer during aging increased the brittleness.

4. CONCLUSION

(1) In the as-reflowed condition, the addition of Zn in excess of 3 wt% eliminated Cu_6Sn_5 at the solder/UBM interface, but precipitated Ag_5Zn_8/Cu_5Zn_8.

(2) Isothermal aging of 0Zn and 1Zn specimens introduced Cu_6Sn_5/Cu_3Sn and Cu_5Zn_8/Cu_6Sn_5 double IMC layers, respectively. In the case of 3Zn and 7Zn specimens, Ag_5Zn_8 decomposed to Cu_5Zn_8 and Ag_3Sn during aging.

(3) Drop resistance (N_f) of Sn-3.5Ag increased about twofold with the addition of 3 wt% Zn, and aging generally deteriorated the drop reliability.

(4) The beneficial role of Zn was ascribed to the suppression of Cu_6Sn_5 formation at the joint interface, and the deleterious effects of aging to the formation of double IMC layers (0Zn, 1Zn) and britlle IMC phases such as Ag_3Sn and Cu_6Sn_5 (3Zn, 7Zn).

ACKNOWLEDGEMENT

This work was supported by the Center for Electronic Packaging Materials (ERC) of MOST/KOSEF (grant #R11-2000-085-05001-0).

REFERENCES

1. J. Muller, H. Griese, and H. Reichl, ICP works '99 in Minneapolis (1999).
2. S. K. Kang and A. K. Sarkhel, *J. Electron. Mater.* **23**, 701 (1994).
3. S. K. Kang, R. S. Rai, and S. Purushothaman, *J. Electron. Mater.* **25**, 1113 (1996).
4. Judith Glazer, *J. Electron. Mater.* **23**, 693 (1994).
5. M. McCorMack and S. Jin, *J. Electron. Mater.* **23**, 715 (1994).
6. W. Yang and R. W. Messler, Jr., *J. Electron. Mater.* **23**, 765 (1994).
7. H. Mavoori, J. Chin, S. Vaynman, B. Moran, L. Keer, and M. E. Fine, *J. Electron. Mater.* **41**, 1269 (1997).
8. T. Takemoto, T. Funaki, and A. Matsunawa, *Welding Res. Abroad* **46,** 20 (2000).
9. K. L. Lin and C. L. Shih, *J. Electron. Mater.* **32**, 95 (2003).
10. K. Suganuma, T. Murata, H. Noguchi, and Y. Toyoda, *J. Mater. Res.* **15**, 884 (2000).
11. K. S. Kim, Y. S. Kim, K. Suganuma, and H. Nakajima, *J. Jpn, Inst. Electron. Packag.* **5**, 666 (2002).
12. Y. Chonan, T. Komiyama, J. Onuki, R. Urao, T. Kimura, and T. Nagano, *Mater. Trans.* **43**, 1887 (2002).
13. T. C. Chang, M. C. Wang, M. S. Hon, *J. Alloys, and Compounds.* **402**, 141 (2005).
14. JEDEC Solid State Technology Association, JESD22-B111, Board Level Drop Test Method of Components for Handheld Electronic Components (2003).
15. W. T. Chen, R. Y. Tsai, Y. L. Lin, and C. R. Kao, *J. Electron. Mater.* **31**, 584 (2002).
16. M. O. Alam, Y. C. Chen, and K. N. Tu, *Chem. Mater.* **15**, 4340 (2003).
17. Y. C. Sohn, Jin Yu, S. K. Kang, D. Y. Shih, and T. Y. Lee, *J. Mater. Res.* **19**, 2428 (2004).
18. Y. C. Sohn and Jin Yu, *J. Mater. Res.* **20**, 1931 (2005).
19. C. E. Ho, R. Y. Tsai, Y. L. Lin, C. R. Kao, *J. Electron. Mater.* **31**, 392 (2002).
20. T. C. Chiu, K. Zeng, R. Strierman, D. Edwards, K. Ano, *ECTC 2004,* p.1256 (2004).
21. J. Yu, Y. C. Sohn, J. Y. Kim, Y. K. Jee, and Y. H. Ko, *ICEP 2006,* p.271 (2006).
22. W. K. Choi, *Ph. D. Thesis,* KAIST (2001).
23. S. K. Kang, D. Leonard, D. Y. Shih, L. Gignac, D. W.

Henderson, S. I. Cho, and J. Yu, *J. Electron. Mater.* **35**, 479 (2006).
24. Massalski, *Binary alloy phase diagram,* vol. 2, pp. 1508-1509.
25. M. Date and K. N. Tu, *J. Mater. Res.* **1**, 2887 (2004).
26. S. P. Yu, M. C. Wang, and M. H. Hon, *J. Mater. Res.* **16**, 76 (2001).
27. S. W. Jeong, J. H. Kim, and H. M. Lee, *J. Electron. Mater.* **33**, 1530 (2004).
28. C. H. Yu and K. L. Lin, *J. Mater. Res*. **20**, 1242 (2005).
29. J. W. Jang, D. Silva. A., J. K. Lin, and D. Frear, *ECTC 2003,* pp. 680-684 (2003).
30. S. K. Kang, P. A. Lauro, D. Y. Shih, D. W. Henderson, and K. J. Puttlitz, *IBM J. RES. & DEV.* **49**, 607 (2005).